



# MIT Open Access Articles

## *Measurement of fragmentation and functionalization pathways in the heterogeneous oxidation of oxidized organic aerosol*

The MIT Faculty has made this article openly available. **Please share** how this access benefits you. Your story matters.

<b>Citation</b>	Kroll, Jesse H. et al. "Measurement of Fragmentation and Functionalization Pathways in the Heterogeneous Oxidation of Oxidized Organic Aerosol." <i>Physical Chemistry Chemical Physics</i> 11.36 (2009): 8005. Web.
<b>As Published</b>	<a href="http://dx.doi.org/10.1039/b905289e">http://dx.doi.org/10.1039/b905289e</a>
<b>Publisher</b>	Royal Society of Chemistry
<b>Version</b>	Author's final manuscript
<b>Citable link</b>	<a href="http://hdl.handle.net/1721.1/71840">http://hdl.handle.net/1721.1/71840</a>
<b>Terms of Use</b>	Creative Commons Attribution-Noncommercial-Share Alike 3.0
<b>Detailed Terms</b>	<a href="http://creativecommons.org/licenses/by-nc-sa/3.0/">http://creativecommons.org/licenses/by-nc-sa/3.0/</a>

1  
2  
3  
4  
5  
6  
7  
8  
9  
10  
11  
12  
13  
14  
15  
16  
17  
18  
19  
20  
21  
22  
23  
24  
25

**Measurement of fragmentation and functionalization pathways  
in the heterogeneous oxidation of oxidized organic aerosol**

Jesse H. Kroll<sup>1,2,3</sup>, Jared D. Smith<sup>4</sup>, Dung L. Che<sup>4,5</sup>, Sean H. Kessler<sup>2</sup>, Douglas R. Worsnop<sup>3</sup>, and Kevin R. Wilson<sup>4\*</sup>

*<sup>1</sup>Department of Civil and Environmental Engineering, Massachusetts Institute of Technology, Cambridge MA 02139; <sup>2</sup>Department of Chemical Engineering, Massachusetts Institute of Technology, Cambridge MA 02139; <sup>3</sup>Center for Aerosol and Cloud Chemistry, Aerodyne Research Inc., Billerica MA 01821; <sup>4</sup>Chemical Sciences Division, Lawrence Berkeley National Laboratory, Berkeley CA 94720; <sup>5</sup>Department of Chemistry, University of California, Berkeley, CA 94720*

\*corresponding author; email KRWilson@lbl.gov, phone 510-495-2474

26 **Abstract**

27

28 The competition between the addition of polar, oxygen-containing functional groups  
29 (functionalization) and the cleavage of C-C bonds (fragmentation) has a governing  
30 influence on the change in volatility of organic species upon atmospheric oxidation, and  
31 hence on the loading of tropospheric organic aerosol. However the relative importance of  
32 these two channels is generally poorly constrained for oxidized organics. Here we  
33 determine fragmentation/functionalization branching ratios for organics spanning a range  
34 of oxidation levels, using the heterogeneous oxidation of squalane ( $C_{30}H_{62}$ ) as a model  
35 system. Squalane particles are exposed to high concentrations of OH in a flow reactor,  
36 and measurements of particle mass and elemental ratios enable the determination of  
37 absolute elemental composition (number of oxygen, carbon, and hydrogen atoms) of the  
38 oxidized particles. At low OH exposures, the oxygen content of the organics increases,  
39 indicating that functionalization dominates, whereas for more oxidized organics the  
40 amount of carbon in the particles decreases, indicating the increasing importance of  
41 fragmentation processes. Once the organics are moderately oxidized ( $O/C \approx 0.4$ ),  
42 fragmentation completely dominates, and the increase in O/C ratio upon further oxidation  
43 is due to the loss of carbon rather than the addition of oxygen. These results suggest that  
44 fragmentation reactions may be key steps in the formation and evolution of oxygenated  
45 organic aerosol (OOA).

46

47 **Introduction**

48

49 The earth's atmosphere contains a huge number of organic compounds, estimated to be in  
50 the tens to hundreds of thousands of individual species<sup>1</sup>. Many, if not most, of these  
51 species are directly involved in the formation and/or evolution of organic particulate  
52 matter, either as precursors to secondary organic aerosol (SOA) or as aerosol components  
53 (or possibly as both). A quantitative and predictive understanding of organic aerosol,  
54 necessary for assessing the role of anthropogenic activity on human health, air quality,  
55 and climate, thus requires a detailed description of the concentrations, properties, and  
56 chemical transformations of a large number of organics. The treatment of so many  
57 species presents substantial challenges for all areas of atmospheric chemistry: the  
58 laboratory study of photochemical reactions, the ambient measurement of atmospheric  
59 concentrations, and the development of accurate chemistry modules for use in chemical  
60 transport models.

61 Rather than attempt to describe all organic species explicitly, many laboratory and  
62 modeling studies treat organic aerosol (and SOA in particular) by lumping organics by  
63 vapor pressure<sup>2,3</sup>. Using this approach, SOA formation is described in terms of only a  
64 few surrogate compounds (two in the case of the "two-product model"<sup>2</sup>, 5-10 in the case  
65 of the "volatility basis set"<sup>3</sup>), substantially simplifying a highly chemically complex  
66 system. The assumption in such a treatment is that the amounts and properties of these  
67 lumped species can be informed by experimental studies of SOA production. However,  
68 laboratory chamber studies generally access initial oxidation reactions only, typically  
69 those that a hydrocarbon undergoes in its first several ( $\leq 12$ ) hours in the atmosphere. By

70 contrast, the atmospheric lifetime of a submicron particle is on the order of 5-12 days<sup>4</sup>,  
71 during which time it may be subject to many more generations of oxidation than are  
72 usually accessed in the laboratory. The products of this additional oxidative processing  
73 are likely to have properties (volatility, solubility, etc.) substantially different than those  
74 generated in chamber studies and included in SOA modules; this disconnect may  
75 contribute to the discrepancies in SOA loading between models and ambient  
76 measurements<sup>5-7</sup>.

77         Recently Donahue et al.<sup>3</sup> suggested that multigenerational oxidation can be  
78 included within lumped SOA modules by use of a “transformation matrix”, which  
79 describes how vapor pressures of (lumped) organic species change upon further  
80 oxidation. However, at present such a matrix can be informed only by chemical intuition  
81 rather than by experimental results, due to the lack of laboratory data constraining the  
82 effects of atmospheric processing on organic volatility. This is a source of significant  
83 uncertainty in models that include the effects of multigenerational oxidation on aerosol  
84 loading<sup>8-10</sup>.

85         An improved treatment of oxidative processing of organics within chemical  
86 transport models requires a quantitative description of how the volatilities of organic  
87 species are affected by atmospheric oxidation reactions. In the gas phase, two main  
88 processes (shown in Figure 1) affect the volatilities of organics: the addition of polar  
89 functional groups, which lowers vapor pressure, and the fragmentation of the carbon  
90 skeleton via C-C bond scission, which increases vapor pressure. (In the condensed phase,  
91 additional bimolecular processes, such as accretion/oligomerization reactions<sup>11-13</sup>, can  
92 also affect volatility.) A key determinant of the changes to the volatility of organic

93 species (and to the loading of organic aerosol) upon atmospheric oxidation is thus the  
94 competition between these functionalization and fragmentation reactions. This is  
95 reasonably well-studied in the case of the oxidation of alkanes, alkenes, and other  
96 reduced organics<sup>14-17</sup>. However, in the case of oxidized species, which make up the  
97 majority of organic particulate matter<sup>18</sup> and which serve as reactants in multigenerational  
98 oxidative processing, the competition between fragmentation and functionalization has  
99 received far less study. This arises in part from experimental constraints, since highly  
100 oxidized atmospheric organics in general are poorly characterized chemically, are present  
101 within complex mixtures, and are not commercially available. The lack of understanding  
102 of the chemical evolution of oxidized organics in the atmosphere severely limits our  
103 ability to accurately model the effects of photochemical processing reactions on  
104 atmospheric organic aerosol.

105         In this work we present the first measurements of the relative importance of  
106 fragmentation and functionalization reactions of organic species spanning a wide range in  
107 oxidation. The chemical system studied is the heterogeneous oxidation of particle-phase  
108 squalane (2,6,10,15,19,23-hexamethyltetracosane, C<sub>30</sub>H<sub>62</sub>) by gas-phase OH radicals.  
109 The heterogeneous oxidation of particulate organics makes for an ideal model system in  
110 that both functionalization and fragmentation reactions can be probed using current  
111 analytical techniques: increases in the oxygen content of the aerosol (as measured by  
112 high-resolution mass spectrometry) indicate functionalization reactions, whereas  
113 decreases in particle mass indicate fragmentation reactions. Squalane particles are  
114 exposed to a very wide range of OH exposures, with upper levels corresponding to  
115 several weeks of atmospheric oxidation. This is more oxidation than particulate organics

116 would experience in their atmospheric lifetimes; however the goal of this high level of  
117 exposure to oxidants is not the simulation of the atmospheric oxidation of reduced  
118 (hydrocarbon-containing) aerosol but rather the generation followed by further oxidation  
119 of highly oxidized organics. This therefore allows for the investigation of  
120 fragmentation/functionalization branching ratios for oxidized chemical species, such as  
121 those in SOA.

122 This work builds directly on our earlier study of the uptake coefficient and  
123 chemical mechanism of the OH + squalane reaction<sup>19</sup>. In that work it was shown that  
124 after substantial oxidation, reactions leading to particle volatilization become important, a  
125 result broadly consistent with results from other heterogeneous oxidation studies<sup>20, 21</sup>.  
126 The present work is aimed at quantifying the importance of such volatilization reactions  
127 as a function of the O/C ratio of the organics, as well as assessing the possible role of  
128 functionalization and fragmentation reactions in the formation of oxidized organic  
129 aerosol (OOA) in the atmosphere.

130

131

## 132 **Experimental**

133

134 The experiments and experimental setup used here are the same as described in Smith, et  
135 al.<sup>19</sup>, so only a brief description is provided here. A simple schematic of the reactor for  
136 the heterogeneous oxidation of organic particles is shown in Figure 2. The flow reactor  
137 consists of a type-219 quartz tube (130 cm long, 2.5 cm ID), with a residence time of 37 s  
138 (total flow 1 liter/min). The carrier flow is N<sub>2</sub>/O<sub>2</sub> (95%/5%), with a water bubbler to

139 keep the flow at 30% relative humidity. Polydispersed submicron squalane particles are  
140 generated upstream of the reactor using a 125°C nucleation oven. The particle size  
141 distribution is log-normal, with a geometric standard deviation of ~1.3, and a mean  
142 surface-weighted diameter of ~160 nm. Ozone (10-200 ppm) is generated upstream by  
143 irradiation of an N<sub>2</sub>/O<sub>2</sub> mixture with Hg pen-ray lamp or a corona discharge ozone  
144 generator (OzoneLab Instruments), and is measured with a commercial ozone monitor  
145 (2B Technologies). Two mercury lamps placed alongside the flow reactor provide 254 nm  
146 light (the quartz blocks shorter UV wavelengths), efficiently photolyzing ozone. The  
147 resulting O(<sup>1</sup>D) reacts with water vapor to generate OH radicals, initiating heterogeneous  
148 reaction. Because of the high water vapor concentrations, O(<sup>1</sup>D) concentrations are  
149 sufficiently low that virtually all oxidation of organics is by the OH radical, with a  
150 negligible (≤1%) contribution by O(<sup>1</sup>D) radicals <sup>19</sup>.

151 OH exposure in the flow tube is monitored using a tracer technique. Small  
152 amounts (75-120 ppb) of hexane are introduced into the tube, and the measurement of the  
153 amount of hexane lost, using a preconcentrator-GC-FID system (SRI Instruments),  
154 enables the determination of the OH concentration<sup>19</sup>. At the highest OH exposures used  
155 here, nearly all of the hexane would be removed if it were allowed to react for the full 37  
156 seconds. Under these conditions the hexane is injected near the end of the flow tube with  
157 a re-entrant tube and so has an OH exposure that is only a fraction of that of the entire  
158 flow tube. The fractional OH exposure is then converted to total OH exposure by a  
159 multiplicative factor. This factor is determined by injecting hexane first into the  
160 beginning of the reactor and then separately through the re-entrant tube at relatively low  
161 OH exposures. Under these conditions OH exposures are low enough that some hexane



162 remains in either case. As we have previously reported,<sup>19</sup> at these low OH exposures the  
163 particle-phase O/C ratios are linearly proportional to the measured OH exposures. Thus  
164 the correction factor is determined by ensuring that the dependence of measured aerosol  
165 O/C ratio (described below) on OH exposure is the same for either configuration (with  
166 and without the re-entrant tube).

167 OH concentrations in the flow tube are controlled by changes to ozone, and range  
168 from  $1.2 \times 10^{10}$  to  $7.4 \times 10^{11}$   $\text{cm}^{-3}$ , several (4-6) orders of magnitude higher than under  
169 typical ambient conditions. If all kinetic processes are first-order with respect to OH,  
170 such differences will not affect the product distribution, since all chemistry will scale  
171 linearly with OH concentration and exposure time. However, processes that are zeroth-  
172 order (such as photolysis) or second-order (such as radical-radical reactions) with respect  
173 to OH could potentially affect product formation in a nonlinear fashion, making  
174 extrapolation down to atmospheric conditions difficult. In a recent study we found little  
175 evidence that such processes play a major role in the chemistry, as products are  
176 essentially unchanged when squalane is exposed to much lower concentrations ( $1-7 \times 10^8$   
177  $\text{cm}^{-3}$ ) of OH, over longer timescales (1.5-3 hours)<sup>22</sup>. At the same time, it was found that  
178 the OH uptake coefficient was somewhat higher at the lower OH concentrations,  
179 suggesting some role of secondary chemistry<sup>22</sup>. The implications of this chemistry for  
180 the extrapolation of flow tube data down to tropospheric conditions will be investigated  
181 in future work.

182 Two instruments are used to characterize the particles exiting the flow reactor, a  
183 scanning mobility particle sizer (SMPS, TSI) and a high-resolution time-of-flight aerosol  
184 mass spectrometer (HR-ToF-AMS, Aerodyne Research<sup>23, 24</sup>). Just prior to measurement

185 by the instruments, the particles are diluted by a factor of ~3-10, in order to keep  
186 measured mass concentrations in the range of 10's-100's of  $\mu\text{g}/\text{m}^3$ . Measurement occurs  
187 within 1-3 seconds after dilution, which is too short for any appreciable repartitioning of  
188 semivolatile species<sup>25</sup>.

189 The AMS is used to measure elemental ratios of the particulate organics. The  
190 instrument used in these experiments has been modified to allow for vacuum ultraviolet  
191 photoionization of the aerosol components<sup>19,26</sup>, but for the experiments described here  
192 only electron impact ionization (EI) is used. Because all ions in the mass spectrum can  
193 be unambiguously identified, high-resolution EI mass spectrometry allows for the  
194 determination of relative abundances of different elements in a sample, namely the  
195 oxygen-to-carbon (O/C) and hydrogen-to-carbon (H/C) molar ratios<sup>27,28</sup>. The intensities  
196 of all organic ions below  $m/z$  100 (including  $\text{CO}_2^+$  and  $\text{CO}^+$ ) are measured directly,  
197 though water-derived ions ( $\text{H}_2\text{O}^+$ ,  $\text{OH}^+$ , and  $\text{O}^+$ ) may also have inorganic sources and so  
198 their contributions to organic signal were estimated using the multiplicative relation  
199 between  $\text{CO}_2^+$  and  $\text{H}_2\text{O}^+$  (0.225) suggested by Aiken, et al.<sup>28</sup> All AMS signal could be  
200 adequately fit by using ions composed only of C, O, and H atoms; as expected, no other  
201 elements were detected in the particles.

202 As demonstrated by Aiken, et al.<sup>27,28</sup>, the elemental ratios determined from EI  
203 need to be corrected for biases arising from ion fragmentation within the mass  
204 spectrometer. Here we apply the empirical multiplicative factor of 1.33 to all O/C  
205 measurements<sup>28</sup>. No correction is applied for the H/C ratio, as the recommended  
206 multiplicative factor (1.1) was found to lead to an overestimate in the H/C ratio for  
207 squalane (and other alkanes). However, since the subsequent data analysis (described in

208 the following section) is mass-based, results are insensitive to this value. These factors  
209 are somewhat uncertain (errors of  $\sim 30\%$ <sup>27</sup>), and may even change with as the aerosol  
210 becomes increasingly oxidized. It is difficult to estimate how such changes might  
211 quantitatively affect our results, but they are unlikely to alter the overall conclusions of  
212 this work. We note that the multiple oxidation reactions form a complex mixture of a  
213 large number of products, for which the correction factors determined by Aiken, et al.<sup>27,28</sup>  
214 are likely to be the most valid, due to the averaging of multiple correction factors for  
215 individual molecules.

216 Particle mass is obtained by combining SMPS and AMS data. Since squalane is a  
217 liquid at room temperature, the particles generated are spherical, enabling a  
218 straightforward calculation of total volume concentrations from SMPS measurements of  
219 size distributions (16-400 nm). Volume concentrations are divided by total particle  
220 number to yield average volume per particle. The ratio of vacuum aerodynamic  
221 diameters (as measured by the AMS<sup>23</sup>) and mobility diameters (as measured by the  
222 SMPS) yields particle density<sup>29</sup>, which when multiplied by SMPS volume gives particle  
223 mass on a per-particle basis. This mass measurement is independent of the collection  
224 efficiency of the AMS, which might change as a function of oxidation.

225 For the experiments reported here, the mass and elemental composition of the  
226 oxidized squalane particles are measured over a wide range of OH exposures. After  
227 several minutes of data collection (corresponding to 1-2 SMPS scans) at a single OH  
228 exposure, the ozone concentration is changed in order to attain a different OH level in the  
229 flow reactor. The system is then allowed to equilibrate for a few minutes before AMS,  
230 SMPS, and GC-FID measurements are made at the new OH exposure. For some

231 experiments the AMS and SMPS are placed downstream of a thermodenuder (TSI,  
232 residence time = 1.6 s), in order to measure particle volatility.

233

234

## 235 **Results**

236

237 Presented in Table 1 and Figure 3 are results from the mass measurements and elemental  
238 analysis of the organic particles as a function of extent of oxidation. Oxidation is  
239 expressed in terms of “squalane oxidation lifetimes”, which is the number of reactions  
240 with OH that an average squalane molecule has undergone; this is equal to the number of  
241 reactive OH collisions with the particle divided by the number of molecules in the  
242 particle<sup>19</sup>. This quantity is not strictly the same as “generation number”, as at any given  
243 time the reaction products will be a statistical mixture of products from different (1<sup>st</sup>, 2<sup>nd</sup>,  
244 3<sup>rd</sup> ...) generations of reaction<sup>19</sup>. The number of squalane lifetimes is given by

$$245 \quad \text{lifetimes} = \frac{\Delta t}{\tau_{sq}} = k[\text{OH}]\Delta t \quad (1)$$

246 in which  $\Delta t$  is exposure time (37s),  $\tau_{sq}$  the timescale of the oxidative loss of squalane,  $k$  is  
247 the measured second-order rate constant, and  $[\text{OH}]$  is the measured concentration of gas-  
248 phase OH. Lifetimes can instead be calculated from particle size, particle density,  
249 uptake coefficient, and molecular weight of the reactive organics<sup>30</sup>, but since we directly  
250 measure the oxidative loss of the squalane<sup>19</sup>, we can determine the value of  $k$  directly  
251 from our experiments and such a calculation is unnecessary. After substantial reaction  
252 (several lifetimes), the squalane molecules will have all reacted away, so “squalane  
253 lifetimes” may no longer accurately describe the average number of reactions the

254 organics have undergone. However this is difficult to correct for, as it requires detailed  
255 characterization of reaction products (with uptake coefficients, molecular weights, etc.),  
256 which is not currently possible. This uncertainty in the degree to which the organics have  
257 reacted with OH does not affect the data or conclusions of this work, though  
258 determination of a simple, size-independent metric for the “extent of oxidation” in a  
259 complex multi-component aerosol would be extremely useful.

260         Measurements of particle volume (normalized to the initial volume per particle of  
261 the unreacted squalane), density, and mass (also normalized) are shown in Figure 3a. At  
262 the initial onset of oxidation, the particle volume increases slightly and then stays roughly  
263 constant with oxidation. Upon further oxidation it then begins decreasing substantially,  
264 by over a factor of 2 at the highest oxidation levels (see Table 1). Density increases  
265 essentially monotonically with oxidation, from  $0.90 \text{ g/cm}^3$  for the unreacted organic to  
266  $1.37 \text{ g/cm}^3$  for the most oxidized organics. This substantial increase in density as the  
267 organics become increasingly oxidized is consistent with measurements of the density of  
268 SOA spanning a range of oxidation levels<sup>31, 32</sup>. The particle mass, determined by  
269 multiplying particle volume by density (and normalizing) increases slightly at first, a  
270 result of the increase in oxygen content of the organics (though the formation of SOA  
271 from the oxidation of squalane vapor may also make a minor contribution). Particle mass  
272 then decreases with further oxidation, indicating volatilization of the organics via  
273 fragmentation reactions. At the highest amount of oxidation studied, the mass per  
274 particle is ~30% lower than for unreacted squalane; however, as noted earlier<sup>19</sup> the total  
275 volatilization of organics is substantially greater than that, since the addition of oxygen  
276 increases the mass of the particles. These results are in agreement with those obtained for

277 the heterogeneous oxidation of bis(2-ethylhexyl) sebacate<sup>20</sup>, though those results covered  
278 a somewhat smaller range in OH exposure and thus less volatilization was observed.

279 Shown in Figure 3b are elemental ratios (O/C and H/C) of the particles, as  
280 determined by the HR-ToF-AMS. The oxygen-to-carbon ratio increases continually as a  
281 function of the extent of oxidation, as expected. The hydrogen-to-carbon ratio initially  
282 decreases, indicating an increase in the degree of unsaturation of the organic molecules,  
283 presumably from the formation of new C-O double bonds in aldehyde and ketone  
284 functional groups. After further oxidation this decrease is less dramatic, suggesting the  
285 increasing importance of C-O single bonds, most likely in carboxylic acid groups.

286 The degree to which functionalization reactions (which add oxygen) and  
287 fragmentation reactions (which remove carbon) occur can be quantified by absolute  
288 molar elemental abundances (the number of atoms of a given element in the particle  
289 phase). These can be calculated from particle mass, which is equal to the sum of the  
290 masses of the elements in the particle (in this case, carbon, oxygen, and hydrogen), and  
291 the measured elemental (H/C and O/C) ratios. Carbon elemental abundance ( $n_C$ ) is  
292 computed as

$$293 \quad n_C = \frac{M}{12 + 16(O/C) + (H/C)} \quad (2)$$

294 in which  $M$  is particle mass and O/C and H/C are molar elemental ratios. Elemental  
295 abundances of oxygen and hydrogen ( $n_O$  and  $n_H$ ) can then be computed from  $n_C$ , O/C,  
296 and H/C. Elemental abundances (normalized to the initial amount of particulate carbon)  
297 are given in Table 2 and Figure 4a. The absolute carbon content increases slightly (~4%)  
298 when oxidation is initiated, which might suggest a minor contribution from SOA formed  
299 by the oxidation of gas-phase squalane. After this initial increase, further oxidation

300 decreases the carbon content, indicating the onset of volatilization reactions; this decrease  
301 becomes quite dramatic after several lifetimes. The oxygen content increases essentially  
302 linearly with oxidation at first, which is consistent with our previous analysis<sup>19</sup>. However  
303 after a few lifetimes this increase in oxygen begins to slow, and stops entirely at high OH  
304 exposure (>10 lifetimes), at which point the absolute oxygen content of the aerosol does  
305 not change with further oxidation. This indicates that the increase in the O/C ratio shown  
306 in Figure 3b is governed not by the addition of oxygen, but instead by the loss of carbon.

307 From these changes in elemental composition upon heterogeneous oxidation, the  
308 branching ratios for fragmentation and functionalization reactions can be calculated.  
309 Assuming that fragmentation reactions are those leading to a decrease in carbon content  
310 (dC), and functionalization reactions are those leading to an increase in oxygen content  
311 (dO), the branching ratio for fragmentation is given by

$$312 \quad \text{BR}_{\text{frag}} = \frac{dC}{dC + dO} = \left(1 + \frac{dO}{dC}\right)^{-1} = \left(1 + \frac{dO/d\tau}{dC/d\tau}\right)^{-1} \quad (3)$$

313 where  $\tau$  is the number of lifetimes (though this calculation is independent of the choice of  
314 oxidation metric). Because the individual measurements are too coarse to permit a  
315 numerical treatment, this expression is evaluated by fitting the data in Figure 4a to simple  
316 functions and differentiating. The functions used are arbitrary ones that fit the data well:  
317  $A_1 + A_2/(\tau^2 + A_3)$  in the case of carbon content and  $A_4(1 - e^{-\tau/A_5})$  in the case of oxygen content  
318 ( $A_n$  values are fitted parameters). This treatment assumes that changes to oxygen and  
319 carbon content result from heterogeneous reactions only. Any gas-to-particle conversion  
320 processes (SOA formation or reactive uptake) would tend to increase the abundance of  
321 both elements in the particles, which would have little effect on Equation 3 unless such

322 processes dominated the chemistry. Such a scenario is highly unlikely given the large  
323 observed decrease in absolute carbon content of the particles (Figure 4a).

324 Computed branching ratios are shown in Figure 4b as a function of O/C ratio of  
325 the organic aerosol. For the least oxidized aerosol (unreacted squalane), functionalization  
326 dominates, with little contribution from fragmentation reactions. Fragmentation becomes  
327 increasingly important for more oxidized organics, and by the time the organics are  
328 moderately oxidized ( $O/C \approx 0.4$ ), fragmentation reactions completely dominate.

329

330

### 331 **Reaction Mechanism**

332

333 The branching ratios between functionalization and fragmentation, shown in Figure 4b,  
334 are determined on an elemental basis and so are not strictly the same as the corresponding  
335 branching ratios between molecular products (Figure 1). For example, multiple atoms  
336 may be involved in a given reaction, with several carbon atoms lost to the gas phase via  
337 fragmentation, or multiple oxygen atoms added in a single functionalization reaction. In  
338 addition, fragmentation reactions might not lead to volatilization if both fragments are  
339 low in vapor pressure; these reactions would not be classified correctly using the present  
340 approach, which is based upon changes to particle mass. Nonetheless, such an atom-  
341 based description is useful for inclusion of multistep oxidation reactions (aging) within  
342 those models that express organic aerosol in terms of the number of carbon and/or  
343 oxygen atoms in the constituent organics<sup>8, 33</sup>.



344 Describing reactions in terms of changes to the bulk elemental composition of  
345 organics provides no molecular information, such as the degree to which individual  
346 organic molecules fragment when particle mass decreases. Shown in Figure 5 are two  
347 general chemical pathways by which volatilization can occur, with decreases in  
348 particulate carbon but no change in particulate oxygen. In pathway 1, both fragmentation  
349 products from the cleavage of the carbon skeleton are volatile and escape to the gas  
350 phase, leading to complete volatilization of the reacted molecule (1a). If this reaction  
351 occurs in parallel with a functionalization reaction (1b), there will be a loss of particulate  
352 carbon but no net change in particulate oxygen. (This pathway includes a  
353 functionalization reaction, but since it involves no change in particulate oxygen, it is  
354 considered a fragmentation reaction using our definition above.) In pathway 2, only one  
355 molecular fragment is volatile (as is the case for small organics, CO, or CO<sub>2</sub>), and  
356 escapes into the gas phase, leading to a loss of particulate carbon. If the amount of  
357 oxygen added to the lower-volatility fragment (which remains in the particle) equals the  
358 amount lost to the gas phase, the net change in particulate oxygen will be zero.

359 These two possibilities do not differ substantially in changes to bulk elemental  
360 composition, but can be distinguished by changes in the volatility of the particulate  
361 organics. In the first pathway (complete volatilization), the organics remaining in the  
362 particle continue to decrease in volatility upon oxidation, as their carbon skeleton remains  
363 intact while polar functional groups are added. In the second (loss of small fragments),  
364 the decrease in volatility from the addition of oxygenated functional groups is offset by  
365 the loss of carbon, so that the overall change in volatility will be minor. Shown in Figure  
366 6 are the results from thermogravimetric (TD) scans, expressed as mass fraction remaining

367 vs. TD temperature, taken at two very different levels of OH exposure. The organics  
368 have undergone substantial oxidation between the two levels (5.1 and 10.1 lifetimes), so  
369 any changes in volatility should be obvious. The curves are almost identical, indicating  
370 that the additional oxidation has little effect on the volatility of the particulate organics.  
371 This suggests that fragmentation occurs via the loss of small volatile fragments from the  
372 organics in the particle (Figure 5, pathway 2). Such a result is qualitatively consistent  
373 with the observation that the gas-phase products of heterogeneous oxidation reactions are,  
374 on average, relatively small (C1-C5)<sup>34, 35</sup>.

375 As discussed in a number of recent studies of the heterogeneous oxidation of  
376 organic species<sup>19-21, 34-39</sup>, the volatilization (fragmentation) of condensed-phase organics  
377 likely arises from the dissociation of alkoxy radical intermediates<sup>14</sup>. The present results  
378 suggest that this dissociation channel dominates in the atmospheric oxidation of relatively  
379 oxidized organics. This is consistent with experimental evidence that oxygen-containing  
380 functional groups (carbonyls and alcohols) greatly increase the rates of alkoxy  
381 fragmentation reactions<sup>14</sup>. It is also consistent with other studies of heterogeneous  
382 oxidation that find evidence of volatilization when oxidation is highest<sup>20, 21</sup>.

383 It should be noted that the fate of alkoxy radicals, and thus the  
384 fragmentation/functionalization branching ratio, is controlled not only by the presence of  
385 oxygen-containing functional groups, but also by structural details of the carbon  
386 skeleton<sup>14, 17</sup>. While the O/C ratios of the reacted organics were varied in this work, the  
387 carbon skeletons were not. Thus the results from this work (Figure 4b) may be most  
388 applicable to organics that have similar structural features to squalane. In particular,  
389 squalane is highly branched, with six tertiary carbons that are expected to have a strong

390 influence on the oxidation chemistry. Their hydrogens are highly susceptible to attack by  
391 OH (relative to primary and secondary hydrogens)<sup>40</sup>, and so tertiary peroxy radicals will  
392 be formed in relatively high yields. In the subsequent RO<sub>2</sub>+RO<sub>2</sub> reaction, the Russell  
393 mechanism<sup>41</sup> is suppressed (due to the lack of α-hydrogens), so tertiary alkoxy radicals  
394 will be the dominant products. These radicals cannot react with O<sub>2</sub> (also due to the lack  
395 of α-hydrogens), and under our experimental conditions appear not to react with other  
396 organics to an appreciable extent<sup>19</sup>, and therefore will mostly dissociate. Thus the  
397 formation and fragmentation of alkoxy radicals is likely a major channel for species with  
398 several tertiary carbons. Compounds which are substantially less branched, such as *n*-  
399 alkanes, may undergo less fragmentation, and thus may have lower fragmentation  
400 branching ratios than those measured in the present study. Nonetheless, even for  
401 unbranched organics, fragmentation is still expected to be a major channel at high O/C  
402 ratios, due to the promotion of alkoxy radical dissociation by oxygen-containing  
403 functional groups.

404         The substantial differences in the chemical composition of organics that have  
405 undergone relatively little heterogeneous oxidation (0-3 lifetimes) versus those that have  
406 undergone substantial oxidation (5+ lifetimes) is illustrated by the evolution of important  
407 AMS marker ions. Shown in Figure 7 are the absolute abundances (mass fraction  
408 multiplied by particle mass) of two ions commonly used as markers for oxidized  
409 organics, C<sub>2</sub>H<sub>3</sub>O<sup>+</sup> (nominal mass *m/z* 43) and CO<sub>2</sub><sup>+</sup> (nominal mass *m/z* 44) as a function  
410 of oxidation lifetimes (CO<sub>2</sub><sup>+</sup> is multiplied by 7 to put the two on the same scale). Also  
411 shown are the amounts of oxygen added and carbon lost from heterogeneous oxidation  
412 (from Table 2; the amount of carbon lost is determined by subtracting the measured

413 carbon content from its maximum value). The increase in  $C_2H_3O^+$  begins immediately  
414 upon oxidation, and closely tracks the amount of oxygen added (functionalization),  
415 whereas the substantial increase in the more heavily oxidized fragment,  $CO_2^+$ , occurs  
416 only after further oxidation and closely follows the amount of carbon lost  
417 (fragmentation). The correlation between individual ions and reaction pathways suggests  
418 that the two may be related, with functionalization reactions forming products that yield  
419 significant  $C_2H_3O^+$  in the mass spectrometer (such as carbonyls), and fragmentation  
420 reactions forming products that yield  $CO_2^+$  (such as acids). This latter observation  
421 suggests that organic acids are formed by reactions associated with C-C bond scission.  
422 One possible mechanism involves acylperoxy ( $RC(O)OO$ ) radicals, which are formed  
423 from the oxidation of aldehydes or the decomposition of alkoxy radicals adjacent to a  
424 carbonyl group<sup>14</sup>, and which will react with  $HO_2$  or  $RO_2$  to form carboxylic acids and/or  
425 peroxyacids. Additionally, the observation of the initial formation of species that yield  
426  $C_2H_3O^+$  ions may help explain why chamber-generated SOA (generally formed after just  
427 a few generations of oxidation) exhibits mass spectra higher in  $m/z$  43 than  $m/z$  44<sup>42, 43</sup>.

428

429

### 430 **Atmospheric Implications**

431

432 This work provides evidence that the cleavage of carbon-carbon bonds (fragmentation) is  
433 an important pathway in the formation of highly oxidized (high O/C) organics via  
434 heterogeneous oxidation. The addition of oxygen-containing functional groups to the  
435 carbon skeleton (functionalization) dominates the heterogeneous oxidation of reduced

436 organic particles throughout their entire atmospheric lifetimes, with fragmentation  
437 reactions being at most a minor channel. However fragmentation is an important  
438 pathway for more oxidized organic species, completely dominating oxidation reactions  
439 for moderately oxidized ( $O/C \approx 0.4$ ) species. Fragmentation leads to the formation of  
440 small, volatile molecules which escape into the gas phase and decrease the carbon content  
441 of the particle. At the same time, oxygen-containing functional groups add to the sites of  
442 the C-C bond breaking, so that the oxygen content of the particulate organics does not  
443 change (Figure 5, pathway 2). As a result, the increase in the O/C ratio of the organic  
444 aerosol upon oxidation is driven not by the addition of oxygen but rather by the loss of  
445 carbon.

446         While the experiments carried out in the present study are focused only on the  
447 heterogeneous oxidation of particulate organics, it is reasonable to infer that  
448 fragmentation may be a key chemical pathway in a wider range of atmospheric oxidation  
449 processes, namely the formation of oxygenated organic aerosol (OOA). OOA is highly  
450 oxidized (with O/C ratios approaching unity<sup>28</sup>), is ubiquitous in the troposphere<sup>18</sup> and  
451 appears to be formed from gas-to-particle conversion (SOA formation) processes<sup>44, 45</sup>.  
452 Since alkoxy radicals are key intermediates in SOA formation<sup>15-17</sup>, the general  
453 conclusions from this work – that oxidized organics fragment upon further oxidation, due  
454 to alkoxy radical decomposition – likely apply to the formation of OOA as well (though  
455 possible differences are described below). The possible link between fragmentation  
456 reactions and OOA formation is supported by the strong correlation between the amount  
457 of carbon lost and the abundance of the  $CO_2^+$  ion (a major tracer for OOA) in the aerosol  
458 mass spectra (Figure 7).

459           These results are consistent with results from several other recent studies which  
460 also point to the importance of fragmentation of organics in the formation of highly  
461 oxidized organics. In the laboratory generation of OOA from the photooxidation of large  
462 (C12 and greater) hydrocarbons, the increase in O/C ratio was found to be much faster<sup>30,</sup>  
463 <sup>46</sup>, and the volatility of the organic aerosol much higher<sup>46</sup>, than what would be expected if  
464 the number of carbon atoms per molecule remained constant. In another study involving  
465 the photooxidation of wood-burning emissions,<sup>47</sup> the O/C ratio (*m/z* 44 mass fraction) of  
466 the aerosol was found to continually increase even though volatility did not change,  
467 which is also seen in the present study (Figure 6). These laboratory studies all suggest  
468 that fragmentation reactions decrease the carbon number of organics during atmospheric  
469 oxidation and OOA formation. Additionally, several recent field studies have shown that  
470 the photochemical processing increases the O/C ratio of the organic aerosol but not the  
471 mass, which necessarily implies a loss of particulate carbon<sup>45, 48, 49</sup>. This may result from  
472 fragmentation reactions of aerosol components, by the gas-phase oxidation of  
473 semivolatiles or, if timescales are long enough, by heterogeneous oxidation<sup>48</sup> (though the  
474 evaporation of organics, coupled with the condensation of highly oxidized organics from  
475 other sources, cannot be ruled out). Taken together, these results suggest that  
476 fragmentation reactions may be key steps in the formation of atmospheric OOA,  
477 implying that the molecules making up OOA may have fewer carbons than their gas-  
478 phase organic precursors.

479           In this work we have presented measurements of the competition between  
480 fragmentation and functionalization channels in atmospheric oxidation (Figure 4b). To  
481 our knowledge this constitutes the first quantitative determination of such branching

482 ratios for organic species spanning a wide range of oxidation; however it should be noted  
483 that these results are not necessarily universal for all organics under all atmospheric  
484 conditions. Deviations from these measured values may result from several factors. (1)  
485 As noted above, structural details of the carbon skeleton have a major influence on  
486 alkoxy radical chemistry. Organics that are significantly less branched than squalane, or  
487 that have other moieties such as double bonds or rings, may have substantially different  
488 fragmentation/functionalization branching ratios<sup>14, 17</sup>. (2) Branching ratios may be  
489 sensitive to reaction conditions, such as NO<sub>x</sub> level, which affects yields of alkoxy  
490 radicals, and aerosol loading, which controls semivolatile partitioning and hence might  
491 affect the degree of volatilization. (3) The 254 nm light used to generate OH may  
492 photolyze oxidized organics (such as carbonyls), which would lead to more  
493 fragmentation than would occur in the ambient atmosphere. (4) Finally, the branching  
494 ratios in the gas phase may be different from those in the present heterogeneous oxidation  
495 experiments, as reactions that occur in one phase may not be important in the other, such  
496 as alkoxy radical isomerization in the gas phase<sup>14</sup>, or reactions between alkoxy radicals  
497 and organic molecules in the condensed phase. In order to obtain a quantitative  
498 understanding of the competition between fragmentation and functionalization reactions  
499 for all atmospheric oxidation processes, these differences need to be explored in future  
500 work. Nonetheless, the present study provides evidence that fragmentation of organics is  
501 an important chemical pathway in the formation of highly oxidized organics (and  
502 particularly OOA) in the atmosphere, and the measured branching ratios provide new  
503 experimental constraints for including the effects of photochemical processing in models  
504 of organic aerosol formation and evolution.

505

506

507 **Acknowledgements**

508 Part of this work was supported by the Director, Office of Energy Research, Office of

509 Basic Energy Sciences, Chemical Sciences Division of the U.S. Department of Energy

510 under Contract No. DE-AC02-05CH11231. J.D.S is supported by the Camille and Henry

511 Dreyfus foundation postdoctoral program in environmental chemistry. D.L.C. is grateful

512 to the National Aeronautics and Space Administration for support on Grant NASA-

513 NNG06GGF26G.

514



515

516 **Table 1.** Changes to aerosol properties upon heterogeneous oxidation.

<b>Life-times</b>	<b>volume (norm.)</b>	<b>density (g/cm<sup>3</sup>)</b>	<b>mass (norm.)</b>	<b>O/C ratio</b>	<b>H/C ratio</b>
0.0	1.00	0.90	1.00	0.00	2.11
0.6	1.02	0.94	1.06	0.03	2.02
1.1	1.02	0.94	1.06	0.05	1.96
1.4	1.00	0.95	1.06	0.06	1.92
1.8	1.00	0.97	1.08	0.08	1.88
3.0	0.93	1.04	1.07	0.11	1.81
3.8	0.89	1.07	1.06	0.14	1.76
4.6	0.86	1.10	1.05	0.17	1.73
6.8	0.78	1.13	0.97	0.23	1.68
8.5	0.74	1.17	0.96	0.26	1.65
9.7	0.71	1.19	0.93	0.28	1.64
10.8	0.68	1.24	0.94	0.29	1.63
11.8	0.66	1.25	0.92	0.31	1.62
12.7	0.64	1.25	0.89	0.32	1.61
14.0	0.62	1.25	0.87	0.33	1.61
15.6	0.59	1.29	0.85	0.35	1.60
16.7	0.58	1.30	0.84	0.36	1.59
25.6	0.49	1.32	0.72	0.42	1.58
35.8	0.46	1.37	0.70	0.45	1.57

517

518

519

520

521 **Table 2.** Absolute elemental composition of heterogeneously oxidized particles and  
522 inferred fragmentation branching ratios.

<b>life-times</b>	<b>carbon content <sup>1</sup></b>	<b>oxygen content <sup>1</sup></b>	<b>hydrogen content <sup>1</sup></b>	<b>branching ratio (fragmentation) <sup>2</sup></b>
0.0	1.00	0.00	2.11	0.00
0.6	1.04	0.03	2.10	0.12
1.1	1.02	0.05	2.00	0.22
1.4	1.00	0.06	1.92	0.28
1.8	1.01	0.08	1.91	0.35
3.0	0.97	0.11	1.75	0.53
3.8	0.93	0.13	1.65	0.61
4.6	0.90	0.16	1.57	0.68
6.8	0.79	0.18	1.33	0.79
8.5	0.76	0.20	1.26	0.84
9.7	0.73	0.20	1.19	0.86
10.8	0.72	0.21	1.18	0.88
11.8	0.70	0.22	1.13	0.89
12.7	0.67	0.21	1.08	0.91
14.0	0.65	0.21	1.05	0.92
15.6	0.63	0.22	1.00	0.93
16.7	0.61	0.22	0.97	0.94
25.6	0.50	0.21	0.79	0.98
35.8	0.48	0.22	0.75	1.00

523

524 <sup>1</sup> absolute molar elemental abundance in the particle, normalized to the amount of carbon  
525 per unreacted squalane particle.

526 <sup>2</sup> see text for details of calculation.

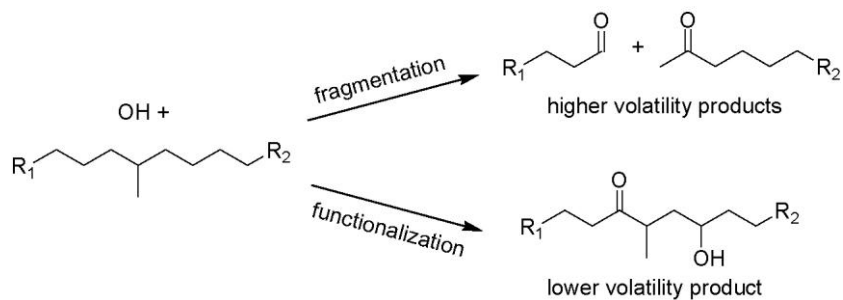
527

528

529

530

531



532

533

534

535 **Figure 1.** Example of fragmentation and functionalization pathways in the atmospheric

536 oxidation of an organic compound. In the oxidation of particulate organics,

537 fragmentation leads to a loss of carbon from the particle (assuming at least one of the

538 fragments is volatile), whereas functionalization leads to an increase in particulate

539 oxygen.

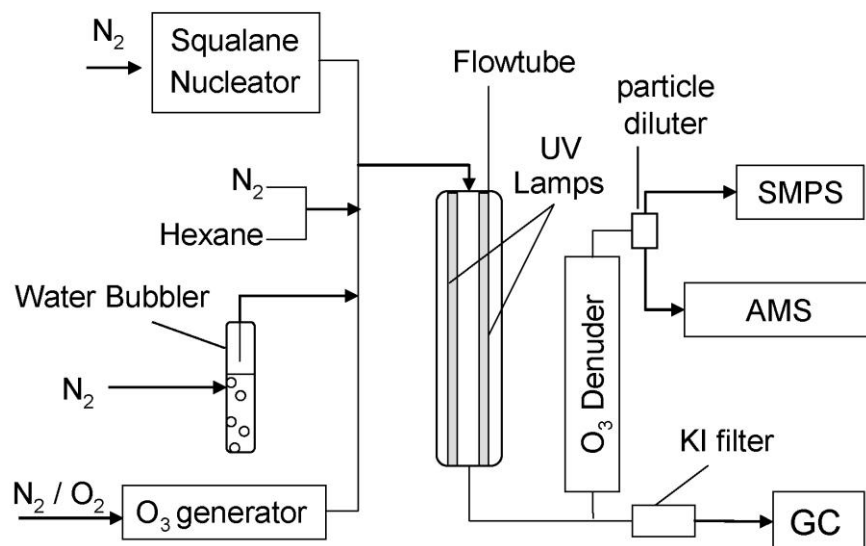
540

541

542

543

544



545

546

547 **Figure 2.** Schematic of the flow reactor used in the present experiments. Squalane

548 particles are generated in a nucleation oven and are exposed to high levels of OH

549 generated from the 254 nm photolysis of ozone in the presence of water vapor. OH

550 concentration is monitored by measuring the loss of a hexane tracer using GC-FID.

551 Reacted particles are characterized using a scanning mobility particle sizer (SMPS) and a

552 high-resolution time-of-flight aerosol mass spectrometer (AMS), for the measurement of

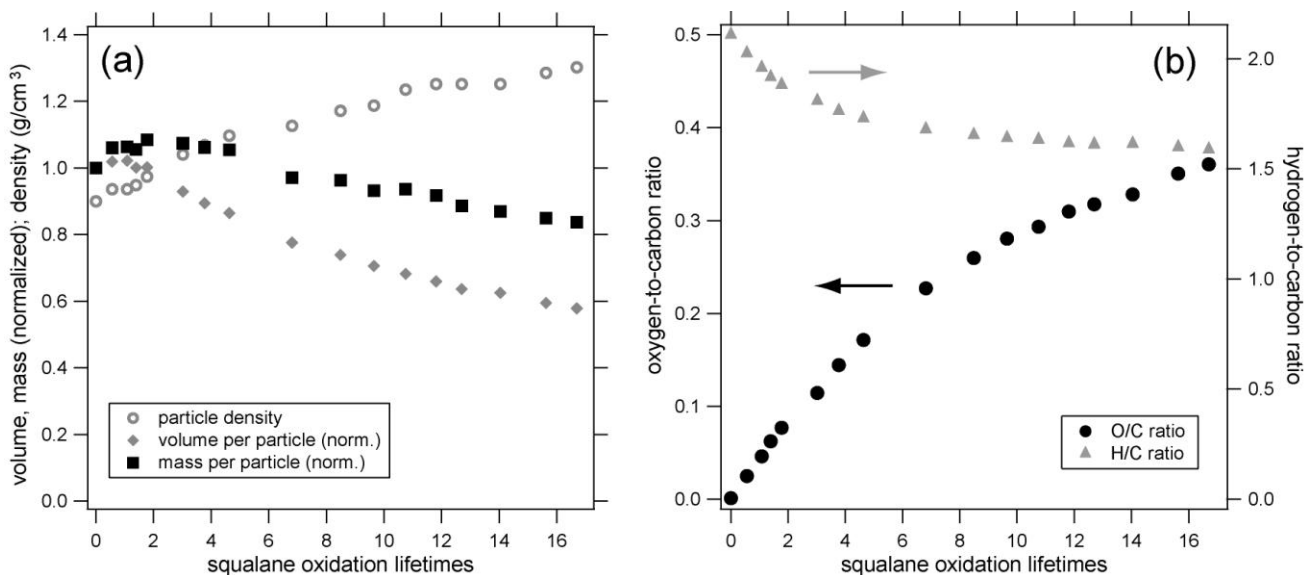
553 particle mass and elemental composition.

554

555

556

557

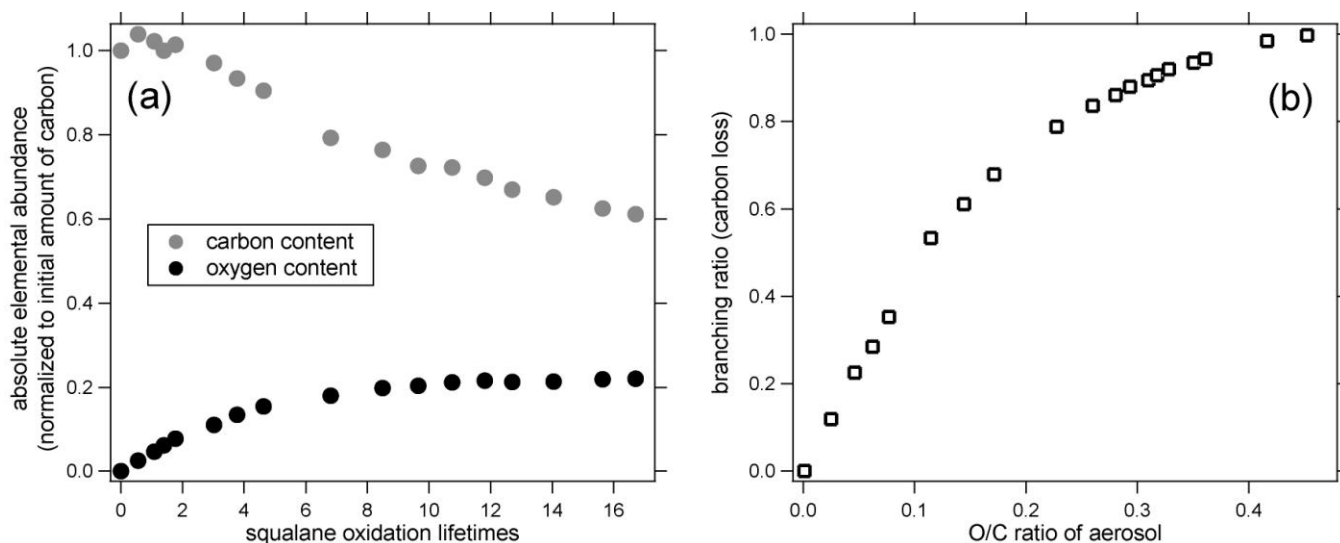


558

559

560 **Figure 3.** Results from AMS and SMPS measurements of the heterogeneously oxidized  
561 particles. *Panel (a)*: particle volume, density, and mass (volume and mass are normalized  
562 to the per-particle values for unreacted squalane). *Panel (b)*: elemental (O/C and H/C)  
563 ratios of organic aerosol. Extent of oxidation (x-axis) is expressed in terms of “squalane  
564 oxidation lifetimes”, which is the number of reactions with OH that an average squalane  
565 molecule has undergone (see text). Not shown: values at the two highest extents of  
566 oxidation, at 25.6 and 35.8 lifetimes (see Table 1 for values).

567



569

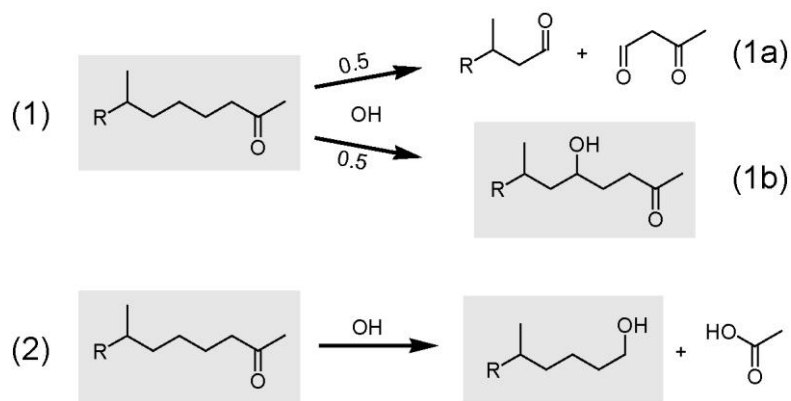
570

571 **Figure 4.** Evolving particle chemistry, as calculated from the measurements of particle  
 572 mass and elemental ratios. *Panel (a)*: absolute molar abundances of carbon and oxygen  
 573 in the particles (normalized to the amount of carbon per unreacted squalane particle). As  
 574 in Figure 3, the two points corresponding to most oxidized organics are not shown (see  
 575 Table 2 for values). With initial oxidation of the squalane, carbon content stays roughly  
 576 constant (the slight increase may be from SOA formation) whereas oxygen content  
 577 increases, indicating the importance of functionalization reactions. Further oxidation  
 578 leads to the loss of carbon from the particles, indicating that fragmentation reactions are  
 579 occurring. The increase in oxygen content then slows and stops completely, and the  
 580 increase in O/C ratio (Figure 3b) is driven entirely by carbon loss. *Panel (b)*: calculated  
 581 branching ratio for the loss of carbon (fragmentation) as a function of O/C ratio of the  
 582 particulate organics. When the aerosol is moderately oxidized (O/C $\approx$ 0.4) fragmentation  
 583 reactions completely dominate. It should be noted that these branching ratios may be  
 584 strongly influenced by the details of the carbon skeleton of squalane; as discussed in the  
 585 “Reaction Mechanism” section, unbranched compounds may undergo substantially less  
 586 fragmentation, particularly at lower O/C ratios.

587

588

589



590

591

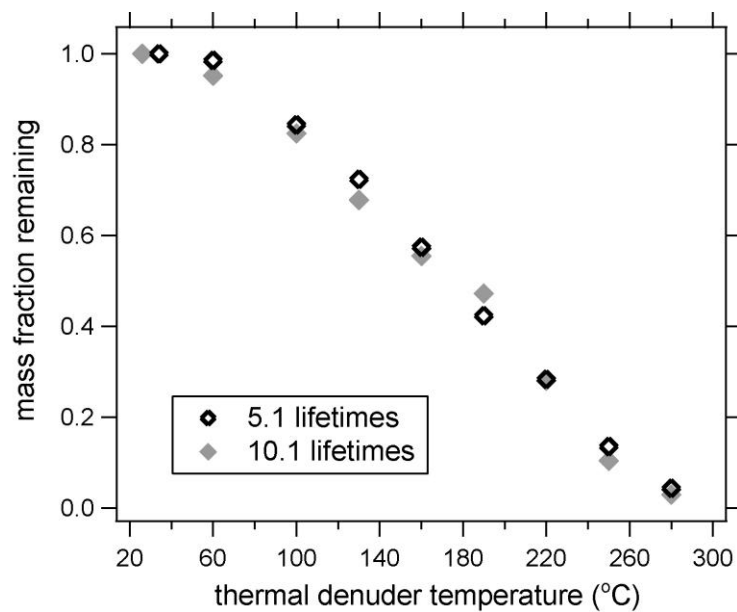
592 **Figure 5.** General oxidative pathways that lead to the loss of particulate carbon but no  
593 change in particulate oxygen. Low-volatility (particle-phase) organics are shaded while  
594 volatile (gas-phase) organics are not. Pathway 1: formation of two volatile fragments  
595 (1a), leading to the complete volatilization of the molecule. If this is accompanied by an  
596 oxygen-addition reaction (1b), total particulate oxygen will stay constant. Pathway 2:  
597 loss of a single volatile species (CO, CO<sub>2</sub>, or small organic) upon fragmentation. A key  
598 difference between the two channels is the volatilities of the particulate products.

599

600

601

602



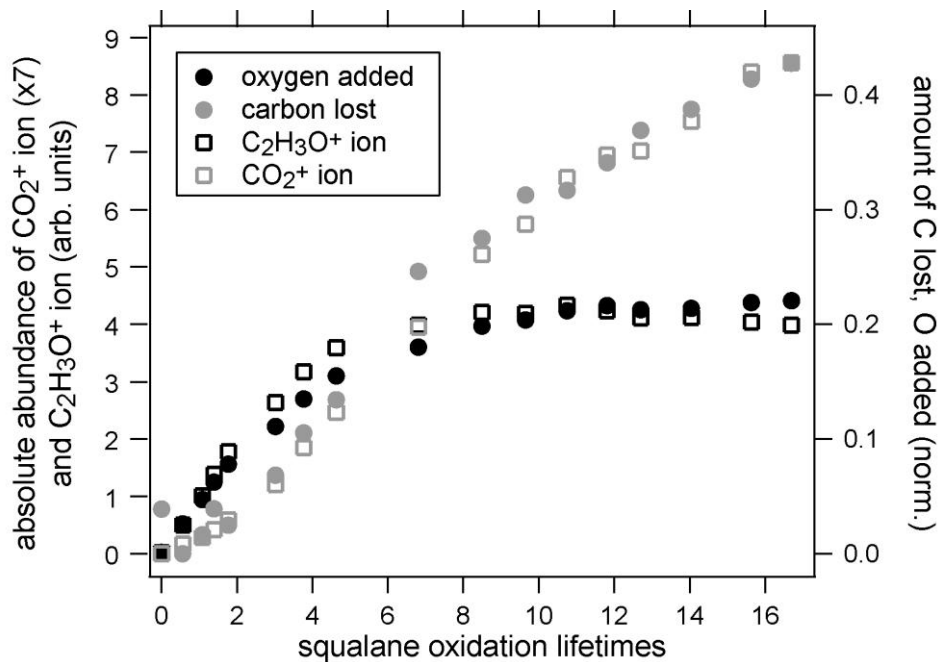
603

604

605 **Figure 6.** Volatility measurements of particulate organics after differing amounts of  
606 heterogeneous oxidation (corresponding to 5.1 and 10.1 lifetimes), obtained by  
607 measuring particle mass downstream of a thermodenuder. The thermograms for the two  
608 lifetimes are nearly identical, indicating the volatilities are similar. This suggests the  
609 importance of the loss of small, volatile fragments from the particulate organics (Figure  
610 5, pathway 2) leading to a decrease in particulate carbon but little change in volatility.



611



612

613

614 **Figure 7.** Absolute abundances of ions used as AMS markers for oxidized organics,

615 CO<sub>2</sub><sup>+</sup> and C<sub>2</sub>H<sub>3</sub>O<sup>+</sup>, as a function of extent of oxidation (shown on the same scale by

616 multiplying CO<sub>2</sub><sup>+</sup> by 7). The two ions track the changing abundances of carbon and

617 oxygen (also shown, right axis), suggesting that C<sub>2</sub>H<sub>3</sub>O<sup>+</sup>, which increases with initial

618 oxidation, may be a marker for functionalization reactions, while CO<sub>2</sub><sup>+</sup>, which increases

619 only with further oxidation, may indicate the importance of fragmentation reactions.

620

621 **References Cited**

- 622 <sup>1</sup> A. H. Goldstein and I. E. Galbally, *Environmental Science and Technology*, 2007,  
623 **41**, 1514.
- 624 <sup>2</sup> J. R. Odum, T. Hoffmann, F. Bowman, D. Collins, R. C. Flagan, and J. H.  
625 Seinfeld, *Environmental Science and Technology*, 1996, **30**, 2580.
- 626 <sup>3</sup> N. M. Donahue, A. L. Robinson, C. O. Stanier, and S. N. Pandis, *Environmental*  
627 *Science and Technology*, 2006, **40**, 2635.
- 628 <sup>4</sup> Y. J. Balkanski, D. J. Jacob, G. M. Gardner, W. C. Graustein, and K. K. Turekian,  
629 *Journal of Geophysical Research-Atmospheres*, 1993, **98**, 20573.
- 630 <sup>5</sup> C. L. Heald, D. J. Jacob, R. J. Park, L. M. Russell, B. J. Huebert, J. H. Seinfeld,  
631 H. Liao, and R. J. Weber, *Geophysical Research Letters*, 2005, **32**, L18809.
- 632 <sup>6</sup> J. A. de Gouw, A. M. Middlebrook, C. Warneke, P. D. Goldan, W. C. Kuster, J.  
633 M. Roberts, F. C. Fehsenfeld, D. R. Worsnop, M. R. Canagaratna, A. A. P.  
634 Pszenny, W. C. Keene, M. Marchewka, S. B. Bertman, and T. S. Bates, *Journal of*  
635 *Geophysical Research-Atmospheres*, 2005, **110**, D16305.
- 636 <sup>7</sup> R. E. Morris, B. Koo, A. Guenther, G. Yarwood, D. McNally, T. W. Tesche, G.  
637 Tonnesen, J. Boylan, and P. Brewer, *Atmospheric Environment*, 2006, **40**, 4960.
- 638 <sup>8</sup> A. L. Robinson, N. M. Donahue, M. K. Shrivastava, E. A. Weitkamp, A. M. Sage,  
639 A. P. Grieshop, T. E. Lane, J. R. Pierce, and S. N. Pandis, *Science*, 2007, **315**,  
640 1259.
- 641 <sup>9</sup> T. E. Lane, N. M. Donahue, and S. N. Pandis, *Atmospheric Environment*, 2008,  
642 **42**, 7439.
- 643 <sup>10</sup> M. K. Shrivastava, T. E. Lane, N. M. Donahue, S. N. Pandis, and A. L. Robinson,  
644 *Journal of Geophysical Research-Atmospheres*, 2008, **113**, DOI:  
645 10.1029/2007JD009735
- 646 <sup>11</sup> K. C. Barsanti and J. F. Pankow, *Atmospheric Environment*, 2004, **38**, 4371.
- 647 <sup>12</sup> M. Kalberer, D. Paulsen, M. Sax, M. Steinbacher, J. Dommen, A. S. H. Prévôt, R.  
648 Fisseha, E. Weingartner, V. Frankevich, R. Zenobi, and U. Baltensperger,  
649 *Science*, 2004, **303**, 1659.
- 650 <sup>13</sup> J. D. Surratt, J. H. Kroll, T. E. Kleindienst, E. O. Edney, M. Claeys, A.  
651 Sorooshian, N. L. Ng, J. H. Offenberg, M. Lewandowski, M. Jaoui, R. C. Flagan,  
652 and J. H. Seinfeld, *Environmental Science and Technology*, 2007, **41**, 517.
- 653 <sup>14</sup> R. Atkinson, *Atmospheric Environment*, 2007, **41**, 8468.
- 654 <sup>15</sup> H. M. Gong, A. Matsunaga, and P. J. Ziemann, *Journal of Physical Chemistry A*,  
655 2005, **109**, 4312.
- 656 <sup>16</sup> Y. B. Lim and P. J. Ziemann, *Environmental Science and Technology*, 2005, **39**,  
657 9229.
- 658 <sup>17</sup> Y. B. Lim and P. J. Ziemann, *Environ. Sci. Technol.*, 2009, **43**, 2328.
- 659 <sup>18</sup> Q. Zhang, J. L. Jimenez, M. R. Canagaratna, J. D. Allan, H. Coe, I. Ulbrich, M. R.  
660 Alfarra, A. Takami, A. M. Middlebrook, Y. L. Sun, K. Dzepina, E. Dunlea, K.  
661 Docherty, P. F. DeCarlo, D. Salcedo, T. Onasch, J. T. Jayne, T. Miyoshi, A.  
662 Shimono, S. Hatakeyama, N. Takegawa, Y. Kondo, J. Schneider, F. Drewnick, S.  
663 Borrmann, S. Weimer, K. Demerjian, P. Williams, K. Bower, R. Bahreini, L.  
664 Cottrell, R. J. Griffin, J. Rautiainen, J. Y. Sun, Y. M. Zhang, and D. R. Worsnop,  
665 *Geophysical Research Letters*, 2007, **34**, L13801.

666 19 J. D. Smith, J. H. Kroll, C. D. Cappa, D. L. Che, C. L. Liu, M. Ahmed, S. R.  
667 Leone, D. R. Worsnop, and K. R. Wilson, *Atmospheric Chemistry and Physics*  
668 *Discussions*, 2009, **9**, 3945.

669 20 I. L. George, A. Vlasenko, J. G. Slowik, K. Broekhuizen, and J. P. D. Abbatt,  
670 *Atmospheric Chemistry and Physics*, 2007, **7**, 4187.

671 21 J. D. Hearn, L. H. Renbaum, X. Wang, and G. D. Smith, *Physical Chemistry*  
672 *Chemical Physics*, 2007, **9**, 4803.

673 22 D. L. Che, J. D. Smith, S. R. Leone, M. Ahmed, and K. R. Wilson, *Physical*  
674 *Chemistry Chemical Physics*, 2009, **THIS ISSUE**.

675 23 J. T. Jayne, D. C. Leard, X. F. Zhang, P. Davidovits, K. A. Smith, C. E. Kolb, and  
676 D. R. Worsnop, *Aerosol Science and Technology*, 2000, **33**, 49.

677 24 P. F. DeCarlo, J. R. Kimmel, A. Trimborn, M. J. Northway, J. T. Jayne, A. C.  
678 Aiken, M. Gonin, K. Fuhrer, T. Horvath, K. Docherty, D. R. Worsnop, and J. L.  
679 Jiménez, *Analytical Chemistry*, 2006, **78**, 8281.

680 25 A. P. Grieshop, N. M. Donahue, and A. L. Robinson, *Geophysical Research*  
681 *Letters*, 2007, **34**, L14810.

682 26 M. J. Northway, J. T. Jayne, D. W. Toohey, M. R. Canagaratna, A. Trimborn, K.  
683 I. Akiyama, A. Shimono, J. L. Jimenez, P. F. DeCarlo, K. R. Wilson, and D. R.  
684 Worsnop, *Aerosol Science and Technology*, 2007, **41**, 828.

685 27 A. C. Aiken, P. F. DeCarlo, and J. L. Jimenez, *Analytical Chemistry*, 2007, **79**,  
686 8350.

687 28 A. C. Aiken, P. F. DeCarlo, J. H. Kroll, D. R. Worsnop, J. A. Huffman, K.  
688 Docherty, I. M. Ulbrich, C. Mohr, J. R. Kimmel, D. Sueper, Q. Zhang, Y. Sun, A.  
689 Trimborn, M. Northway, P. J. Ziemann, M. R. Canagaratna, R. Alfarra, A. Prevot,  
690 J. Dommen, J. Duplissy, A. Metzger, U. Baltensperger, and J. L. Jiménez,  
691 *Environ. Sci. Technol.*, 2008, **42**, 4478.

692 29 P. DeCarlo, J. G. Slowik, D. R. Worsnop, P. Davidovits, and J. L. Jiménez,  
693 *Aerosol Sci. Tech.*, 2004, **38**, 1185–1205.

694 30 A. L. Robinson, N. M. Donahue, and W. F. Rogge, *Journal of Geophysical*  
695 *Research-Atmospheres*, 2006, **111**, D03302.

696 31 J. E. Shilling, Q. Chen, S. M. King, T. Rosenoern, J. H. Kroll, D. R. Worsnop, P.  
697 F. DeCarlo, A. C. Aiken, D. Sueper, J. L. Jimenez, and S. T. Martin, *Atmospheric*  
698 *Chemistry and Physics*, 2009, **9**, 771.

699 32 J. E. Shilling, Q. Chen, S. M. King, T. Rosenoern, J. H. Kroll, D. R. Worsnop, K.  
700 A. McKinney, and S. T. Martin, *Atmospheric Chemistry and Physics*, 2008, **8**,  
701 2073.

702 33 J. F. Pankow and K. C. Barsanti, *Atmos. Environ.*, 2009, **43**, 2829.

703 34 M. J. Molina, A. V. Ivanov, S. Trakhtenberg, and L. T. Molina, *Geophysical*  
704 *Research Letters*, 2004, **31**, L22104.

705 35 A. Vlasenko, I. J. George, and J. P. D. Abbatt, *Journal of Physical Chemistry A*,  
706 2008, **112**, 1552.

707 36 T. L. Eliason, J. B. Gilman, and V. Vaida, *Atmospheric Environment*, 2004, **38**,  
708 1367.

709 37 K. S. Docherty and P. J. Ziemann, *Journal of Physical Chemistry A*, 2006, **110**,  
710 3567.

711 38 D. A. Knopf, J. Mak, S. Gross, and A. K. Bertram, *Geophysical Research Letters*,  
712 2006, **33**, L17816.  
713 39 V. F. McNeill, R. L. N. Yatavelli, J. A. Thornton, C. B. Stipe, and O. Landgrebe,  
714 *Atmospheric Chemistry and Physics*, 2008, **8**, 5465.  
715 40 E. S. C. Kwok and R. Atkinson, *Atmospheric Environment*, 1995, **29**, 1685.  
716 41 G. A. Russell, *J. Am. Chem. Soc.*, 1957, **79**, 3871–3877.  
717 42 R. Bahreini, M. D. Keywood, N. L. Ng, V. Varutbangkul, S. Gao, R. C. Flagan, J.  
718 H. Seinfeld, D. R. Worsnop, and J. L. Jimenez, *Environmental Science and*  
719 *Technology*, 2005, **39**, 5674.  
720 43 M. R. Alfarra, D. Paulsen, M. Gysel, A. A. Garforth, J. Dommen, and A. S. H.  
721 Prévôt, Worsnop, D. R., Baltensperger, U., Coe, H., *Atmospheric Chemistry and*  
722 *Physics*, 2006, **6**, 5279.  
723 44 Q. Zhang, D. R. Worsnop, M. R. Canagaratna, and J. L. Jimenez, *Atmospheric*  
724 *Chemistry and Physics*, 2005, **5**, 3289.  
725 45 P. F. DeCarlo, E. J. Dunlea, J. R. Kimmel, A. C. Aiken, D. Sueper, J. Crouse, P.  
726 O. Wennberg, L. Emmons, Y. Shinozuka, A. Clarke, J. Zhou, J. Tomlinson, D. R.  
727 Collins, D. Knapp, A. J. Weinheimer, D. D. Montzka, T. Campos, and J. L.  
728 Jimenez, *Atmospheric Chemistry and Physics*, 2008, **8**, 4027.  
729 46 A. A. Presto, M. A. Miracolo, N. M. Donahue, A. L. Robinson, J. H. Kroll, and D.  
730 R. Worsnop, *Environ. Sci. Technol.*, 2009, **in press**.  
731 47 A. P. Grieshop, N. M. Donahue, and A. L. Robinson, *Atmospheric Chemistry and*  
732 *Physics Discussions*, 2008, **8**, 17095.  
733 48 E. J. Dunlea, P. F. DeCarlo, A. C. Aiken, J. R. Kimmel, R. E. Peltier, R. J. Weber,  
734 J. Tomlinson, D. R. Collins, Y. Shinozuka, C. S. McNaughton, S. G. Howell, A.  
735 D. Clarke, L. K. Emmons, E. C. Apel, G. G. Pfister, A. van Donkelaar, R. V.  
736 Martin, D. B. Millet, C. L. Heald, and J. L. Jimenez, *Atmospheric Chemistry and*  
737 *Physics Discussions*, 2008, **8**, 15375.  
738 49 G. Capes, B. Johnson, G. McFiggans, P. I. Williams, J. Haywood, and H. Coe,  
739 *Journal of Geophysical Research-Atmospheres*, 2008, **113**, DOI:  
740 10.1029/2008JD009845  
741  
742